Journal of Power Technologies 104 (3) (2024) 189 -- 200

Energy and exergy analyses of an advanced combined cycle fired by natural gas and biomass

S.S. Laleh [1], S.M.S Mahmoudi [1], S. Soltani [2] ✉, T. Morosuk [3]

[1] University of Tabriz, Faculty of Mechanical Engineering, 16471 Tabriz, Iran
[2] Antalya Bilim University, Faculty of Engineering and Natural Sciences, 07190 Antalya, Turkey
[3] Technical University of Berlin, Institute for Energy Engineering, March Str 18, 10587 Berlin, Germany

✉ soltani929@gmail.com; saeed.soltani@antalya.edu.tr

Abstract

A modified combined cycle with an intercooler and a reheater (CCIR) within the gas-turbine system is proposed and evaluated. The fuel for the combustion chamber is natural gas, and the fuel for the reheater is provided by gasified biomass. Adding an intercooler between two compressors and a preheater for the compressed air before entering the combustion chamber increases the efficiency of the overall system. A further increase in efficiency was achieved through the utilization of the heat of the exiting hot gases in a Rankine cycle. The system has a fixed power output of 10 MW. The system's improvements resulted in 56.3% of the overall energy efficiency and 50.7% of the exergy efficiency. Natural gas and biomass flow rates are 0.139 kg/s and 0.776 kg/s, respectively.

Introduction

Fossil fuels are a limited energy source and, more importantly, their excessive negative impact on the environment and global warming is the more notable one [1,2,3]. The finite nature of these fossil fuel resources bestows upon them a dual characterization, embodying both scarcity and substantial ecological liabilities. Nonetheless, an immediate and complete disavowal of fossil fuels remains impractical, necessitating a protracted and intricate voyage toward attaining wholly carbon-neutral energy paradigms [4]. Within the spectrum of accessible fossil fuels, natural gas has emerged as a frequently tapped resource for generating electricity [5, 6], and is a very effective technology, particularly for the application in combined cycles.

Modifications can be applied to a simple gas-turbine system to achieve a higher performance. Adding intercoolers, reheaters, and regenerators can be very effective. The gas-turbine system can be substantially improved when the intercooler, reheater, and preheater are involved simultaneously [7,8].

Heat recovery through adding a power generation unit is another way to increase overall efficiency. A steam cycle is the concept of industrial large-capacity combined-cycle power plants. The application of the organic Rankine cycle (ORC) including sCO_2 as the working fluid, can be considered for medium- and small-scale applications, and already has proven to be one of the more efficient options [9,10]. To further increase the sustainability of the system, i.e., decrease CO_2 emissions and implement renewables, the authors proposed using biomass as a fuel for reheating. Biomass is widely regarded as an accessible and cheap energy source [11,12,13]. There are many possibilities to use biomass as a fuel for power plants. Despite the several benefits of biomass gasification, it still lags in commercialization due to its specific technological, implementation, and policy challenges. Because of the fuel flexibility for gasification, many gasification technologies, and corresponding capacities can be used for different industries and conditions [14,15,16,17]. The gasifier considered in this paper is thoroughly studied and compared with other options published by Soltani et al. [18,19,20,21, 22].

The proposed system is a modified combined cycle (CCIR) that includes two-stage compression with an intercooler and a reheater combustion chamber (RCC) in addition to the main combustion chamber (CC). Natural gas is the fuel for the CC, and a biomass gasifier provides fuel for RCC. Having different fuels gives the flexibility of fuel management to the system. A thermodynamic (energy and exergy) analysis is carried out to demonstrate the advantages of the CCIR system.

Materials and methods

Schematic of CCIR

The CCIR system (Figure 1) comprises the topping and bottoming cycles. The topping cycle is an open-cycle gas-turbine system with an intercooler between two stages of compression, a preheater, and a reheater between two turbines. In the topping cycle, air enters the first compressor (C1) under environmental conditions (state 1). Air compressed with the pressure ratio of rp1 and cooled down in an IC (state 3). In the second compression stage, the air is compressed (C2) with the pressure ratio of rp2 (state 4). Compressed air gets heated (state 5) by the combustion gases after the second turbine (T2) and before entering the combustion chamber (CC). State 6 is the stream of combustion gas at TIT. After expansion in T1, combustion gases have reached state 7. State 8 is the combustion gases after the reheating within the second combustion process.

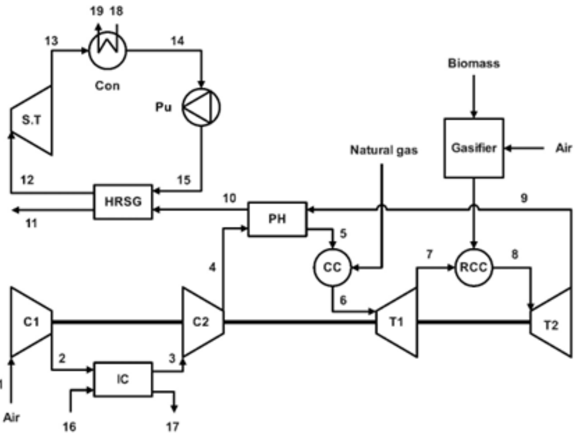

Figure 1 Schematic of CCIR system.

At state 10, the combustion gases are entering the heat recovery steam generator (HRSG). The bottoming cycle is a simplified Rankine cycle [18,19].

Assumptions

Environmental air is assumed to be a mixture of 79 mol% nitrogen and 21 mol% oxygen. The combustion processes at CC and RCC are considered adiabatic. The pressure drops in CC, RCC, PH, IC, and HRSG are neglected, and the cooling water's temperature in IC and Con increases by 10 K. The assumptions for simulation are listed in Table 1.

Energy and exergy analyses of components

Thermodynamic assessment of the CCIR system consists of energy and exergy balances (Table 2). For the steady-state operation:

- mass balance

$$\sum \dot{m}_{in} = \sum \dot{m}_{out}$$

- energy balance

$$\sum \dot{m}_{out} h_{out} - \sum \dot{m}_{in} h_{in} = \dot{Q} - \dot{W}$$

- overall energy efficiency

$$\eta = \frac{\dot{W}_{net}}{\sum \dot{m}_{Fuel} LHV_{Fuel}}$$

- exergy balance is conducted in the terms "exergy in / exergy out"

$$\dot{E}_D = \dot{E}_i - \dot{E}_{out}$$

- overall exergy efficiency

$$\varepsilon = \frac{\dot{W}_{net}}{\sum \dot{E}_{Fuel}}$$

Biomass gasification process

The considered gasifier is a downdraft. The reaction zones of a downdraft gasifier from top to bottom are four, namely drying, pyrolysis, oxidation, and reduction zones [23]. Biomass is wood, consisting of carbon, hydrogen, and oxygen with moisture content. The percentages of each substance are 50%, 6%, and 44%, respectively; also, moisture content of wood is 20% and is measured by weight [24,25].

Table 1 Parametric assumptions and initial data (based on [18-22]).

Variable Name	Unit	Value
P1	kPa	101.3
T1	K	298
T3	K	318
r_{p1}	-	4.5
r_{p2}	-	11
TIT for T1 and T2	K	1400-1500
Tg	K	1073
T10	K	960
T12	K	800
Maximum/minimum pressure of the bottoming cycle	kPa	8104 / 8.104
$\eta_{is,C}$	-	0.87
$\eta_{is,T}$	-	0.89
$\eta_{is,ST}$	-	0.9
$\eta_{is,Pu}$	-	0.8
Pinch point temperature difference in HRSG	K	10
Net power output	MW	10

The overall equation of the gasification reaction for one carbon atom is:

$$CH_XO_YN_Z + wH_2O + m(O_2 + 3.76N_2) \rightarrow n_1H_2 + n_2CO + n_3CO_2 + n_4H_2O + n_5CH_4 + n_6N_2$$

where "w" is the amount of moisture per kmol of wood and "m" is the amount of oxygen per kmol of wood for the gasification process. Equations to calculate the thermodynamic parameters of the biomass, like higher heating value (HHV), lower heating value (LHV), MC, and $\dot{E}_{biomass}$, can be found, for example, in [26,27].

Results and discussion

A sensitivity analysis is applied to different operation parameters of the system for a comprehensive thermodynamic evaluation of the CCIR system. This study aims to select the combination of parameters that correspond to the maximum overall energy efficiency and, therefore, minimum cumulative fuel consumption. Three key parameters of the topping cycle are selected: TIT, r_{p1}, and r_{p2} (Figure 2, Table 3).

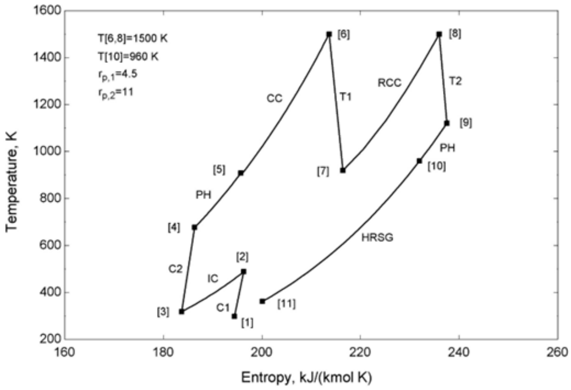

Figure 2 T-s diagram of the topping cycle at given parameters.

Energy analysis

Figure 3 demonstrates the effect of r_{p1} on the overall energy efficiency for two selected values of TIT. The value of r_{p1} is assumed to be varied in the limit between 3 and 7. The maximum value of efficiency is observed at the same pressure ratio r_{p1}.

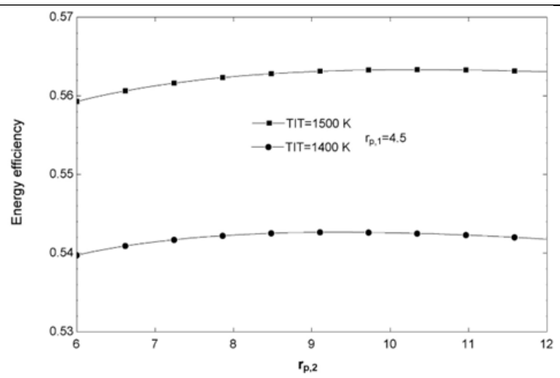

Figure 3 Energy efficiency vs. rp2 for two values of TIT.

Table 2: Definitions for energy and exergy balances for the CCIR components.

Component	Energy balance	Max P, MPa
C1	$\dot{W}_{C1} = \dot{n}_1 h_1 - \dot{n}_2 h_2$	$\dot{E}_1 - \dot{E}_2 - \dot{W}_{C1}$
C2	$\dot{W}_{C2} = \dot{n}_3 h_3 - \dot{n}_4 h_4$	$\dot{E}_3 - \dot{E}_4 - \dot{W}_{C2}$
IC	$\dot{n}_2 h_2 - \dot{n}_3 h_3 = \dot{n}_{17} h_{17} - \dot{n}_{16} h_{16}$	$\dot{E}_2 - \dot{E}_3 + \dot{E}_{16} - \dot{E}_{17}$
PH	$\dot{n}_5 h_5 - \dot{n}_4 h_4 = \dot{n}_9 h_9 - \dot{n}_{10} h_{10}$	$\dot{E}_4 - \dot{E}_5 + \dot{E}_9 - \dot{E}_{10}$
CC	$\dot{n}_5 h_5 - \dot{n}_{nat\ gas} h_{nat\ gas} = \dot{n}_6 h_6$	$\dot{E}_5 + \dot{E}_{nat\ gas} - \dot{E}_6$
T1	$\dot{W}_{T1} = \dot{n}_6 h_6 - \dot{n}_7 h_7$	$\dot{E}_6 - \dot{E}_7 - \dot{W}_{T1}$
RCC	$\dot{n}_7 h_7 + \dot{n}_{BF} h_{BF} = \dot{n}_8 h_8$	$\dot{E}_7 + \dot{E}_{BF} - \dot{E}_8$
T2	$\dot{W}_{T2} = \dot{n}_8 h_8 - \dot{n}_9 h_9$	$\dot{E}_8 - \dot{E}_9 - \dot{W}_{T2}$
HRSG	$\dot{n}_{10} h_{10} - \dot{n}_{11} h_{11} = \dot{n}_{12} h_{12} - \dot{n}_{15} h_{15}$	$\dot{E}_{10} - \dot{E}_{11} + \dot{E}_{15} - \dot{E}_{12}$
ST	$\dot{W}_{ST} = \dot{n}_{12} h_{12} - \dot{n}_{13} h_{13}$	$\dot{E}_{12} - \dot{E}_{13} - \dot{W}_{ST}$
Con	$\dot{n}_{13} h_{13} - \dot{n}_{14} h_{14} = \dot{n}_{19} h_{19} - \dot{n}_{18} h_{18}$	$\dot{E}_{13} - \dot{E}_{14} + \dot{E}_{18} - \dot{E}_{19}$
Pu	$\dot{W}_{PU} = \dot{n}_{14} h_{14} - \dot{n}_{15} h_{15}$	$\dot{E}_{12} - \dot{E}_{13} - \dot{W}_{PU}$

The second compressor has similar behavior (Figure 4); however, the value of r_{p2} is assumed to be varied in the limit between 6 and 12.

Figure 5. demonstrates the effect of rp1 on natural gas and biomass consumption in CC and RCC for TIT=1500K. As rp1 increases, the amount of required biomass decreases; contrarily, natural gas consumption increases as rp1 increases. Note that the value of rp2 is fixed. Therefore, natural gas and biomass consumption variations to rp2 will be the opposite. The same character of curves is observed for the effect of rp2 on natural gas and biomass consumption (Figure 6). Figure 7 demonstrates the sensitivity analysis results at rp1 = rp2 (in the range between 3 and 7).

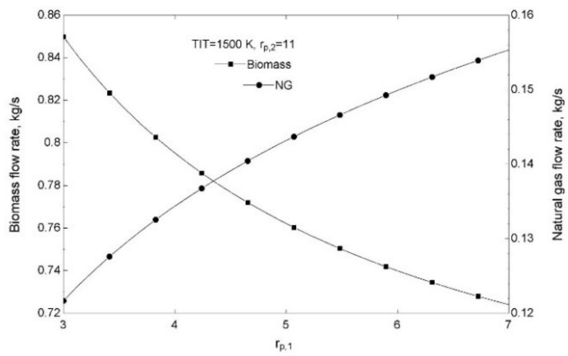

Figure 4 Biomass and the natural gas flow rate vs. rp1.

Table 3: Thermodynamics characteristics at states in CCIR system.

State	Temperature, K	Pressure, kPa	Specific enthalpy, kJ/kmol	Specific entropy, kJ/kmolK	Specific exergy, kJ/kmol
1	298	101.3	-4	194.3	0
2	488.1	455.9	5595	196.3	5000
3	318.0	455.9	578	183.7	3746
4	676.6	5014	11343	186.3	13724
5	908.7	5014	18731	195.7	18317
6	1500.0	5014	16214	213.6	34025
7	919.9	455.9	-4133	216.4	12828
8	1500.0	455.9	-19119	235.9	29236
9	1121.0	101.3	-33331	237.5	14547
10	960.0	101.3	-39094	231.9	10437
11	361.4	101.3	-58847	200.1	181
12	800.0	8104	62412	122.6	25968
13	314.9	8.104	40772	130.2	2053
14	314.9	8.104	3150	10.7	33
15	315.6	8104	3334	10.8	182

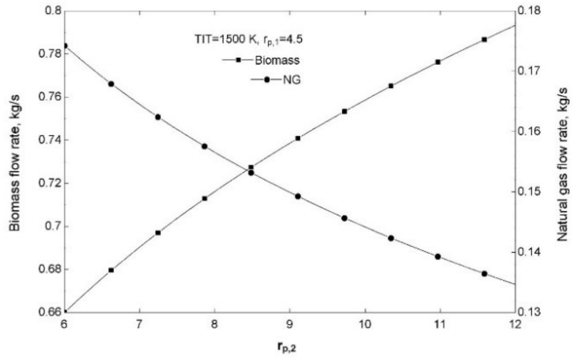

Figure 5 Biomass and the natural gas flow rate vs. rp2.

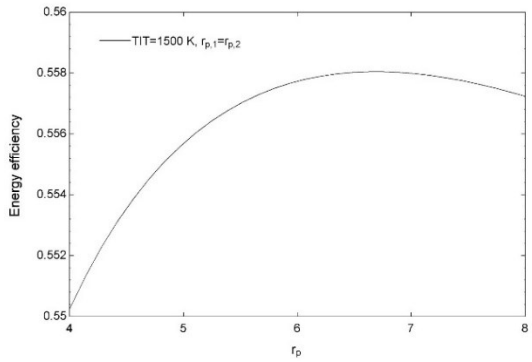

Figure 6 Variations of energy efficiency of the system at rp1 = rp2.

Increasing the value of TIT for both turbines results in the fuel consumption for CC and RCC. Therefore, the natural gas flow rate for CC decreases, and the biomass flow rate for RCC increases to maintain the required temperature, as is shown in Figure 8.

The effect of a bottoming cycle on the overall energy efficiency and the evaluated combined cycle at different TIT is shown in Figure 9.

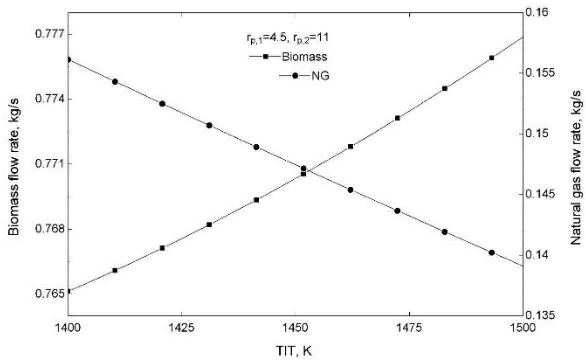

Figure 7 Biomass and the natural gas consumption vs. TIT.

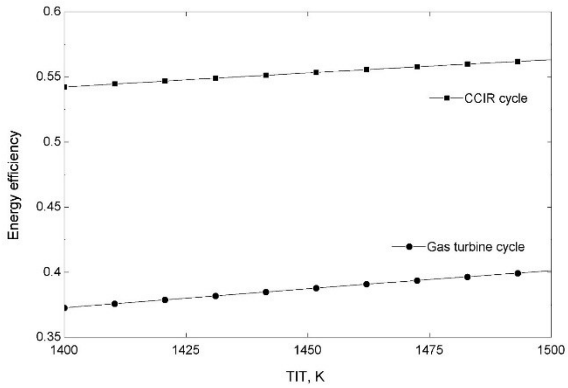

Figure 8 Comparison of variations of CCIR and gas turbine cycle versus TIT.

In addition to efficiency, the CO2 emissions as an important variable for the ecological evaluation of a power plant are evaluated. Here, the amount of generated CO2 has been calculated at r_{p1}=var, r_{p2}=var, and TIT=var (Figure 10).

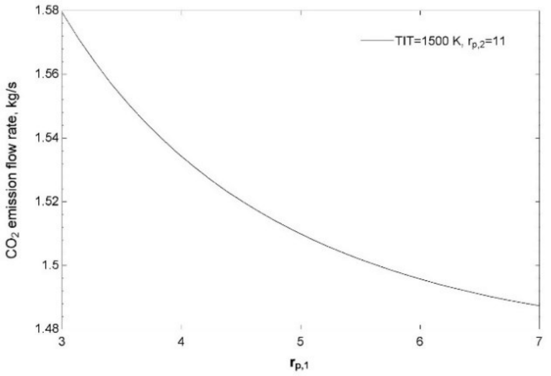

a)

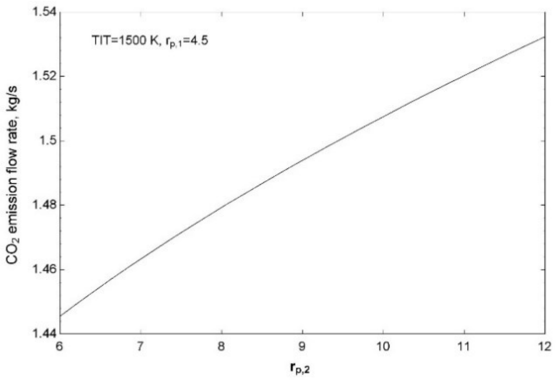

b)

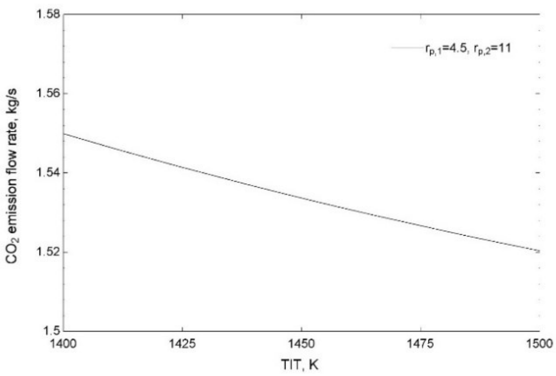

c)

Figure 9 CO2 emissions vs. a) rp1, b) rp2, and c) TIT.

Exergy analysis

An exergy sensitivity analysis has been conducted in analogy to energy sensitivity analysis. The exergetic variables are overall exergy efficiency and the total exergy destruction (Figure 11 through 14).

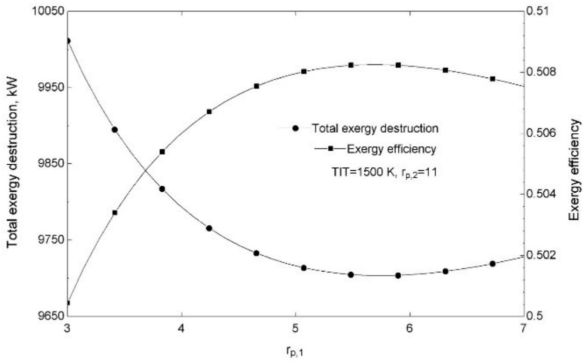

Figure 10 Total exergy destruction and exergy efficiency vs. rp1.

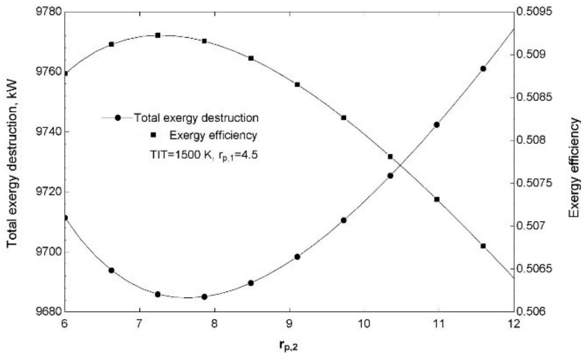

Figure 11 Total exergy destruction and exergy efficiency vs. rp2.

Figure 12. demonstrates the effect of TIT on exergy efficiency and the total exergy destruction in the system. Increasing the amount of TIT for turbines increases the exergy efficiency of the system, and consequently, exergy destruction of the system decreases. Increasing the amount of TIT has a similar effect on the total exergy loss of the system, as shown in Figure 13.

The exergy analysis results on a component level are given in Figure 15 through 17. The total exergy destruction is 9742 kW. The interstage cooler (IC) in the gas-turbine system and the condenser (Con) in the Rankine cycle are considered as dissipative components.

The value of exergy destruction with the pump of the Rankine cycle is negligibly small. Note that 39% of the total exergy destruction, 3824 kW, is associated with the gasifier (Ga).

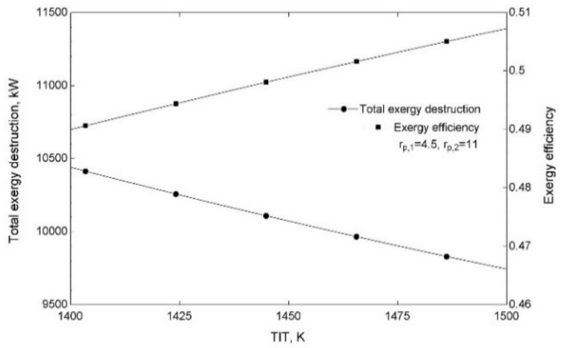

Figure 12 Total exergy destruction and exergy efficiency vs. TIT.

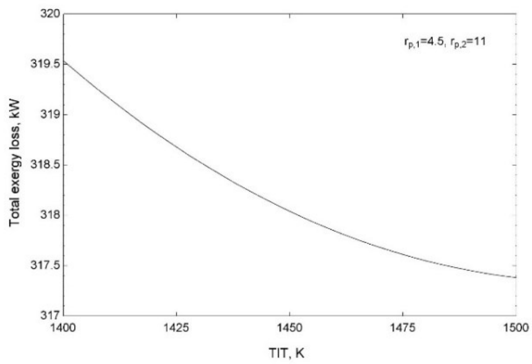

Figure 13 Total exergy loss versus TIT.

The exergy efficiency of CCIR components, shown in Figure 16, is higher than similar values calculated using the approach of exergy of fuel/exergy of product.

Nevertheless, the gasifier has the lowest exergy efficiency among system components (70%).

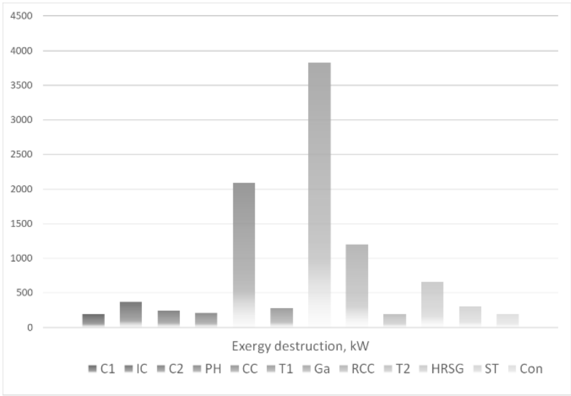

Figure 14 Exergy destruction rates within CCIR components (except Pu).

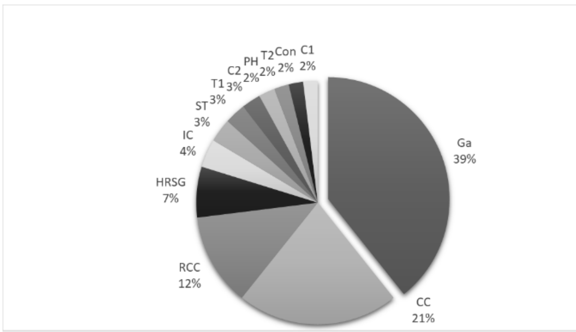

Figure 15 The contribution of the exergy destruction rates within CCIR components (except Pu).

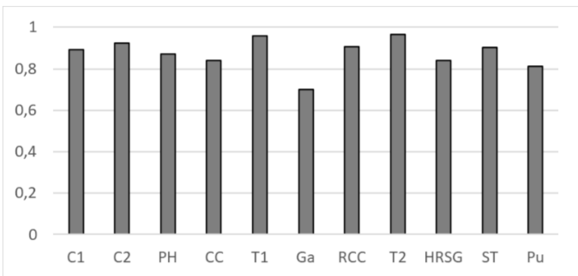

Figure 16 Exergy efficiency of CCIR components (except IC and Con).

Discussions and conclusion

A theoretical study of an advanced combined cycle is conducted. The gas-turbine system with an intercooler and reheater is fired by natural gas and gasified biomass. Such a system can be considered for a small- or medium-scale application. As an academic example, a power generation of 10 MW was assumed.

The results of the parametric sensitivity analysis show that the maximum values of the energy and exergy efficiency of the system are observed at slightly different operation conditions for the compression processes: r_{p1}=4.5 and r_{p2}=11 from the energetic evaluation and r_{p1}=5.5 and r_{p2}=7 from exergetic evaluation. Also, increasing the TIT correlates with increased energy and exergy efficiency. For the selected operation conditions (considered after evaluation of the sensitivity analysis results), the overall system can achieve 56.3% energy efficiency and 50.7% exergy efficiency. Also, the CO_2 emissions are calculated as 1.52 kg/s. The bottoming cycle generates 2.9 MW of power (approximately 1/3 of the total value). Without this waste heat recovery, the energy and exergy efficiency of the system would have dropped to 40.1% and 36.1%, respectively.

Author contributions: Shayan Sharafi Laleh: Conceptualization, Methodology, software, investigation, writing—original draft preparation, S.M.S Mahmoudi: Methodology, Supervision, Saeed Soltani: Methodology, Supervision; Tatiana Morosuk: Supervision, Methodology.

Funding: This research received no external funding. Conflicts of interest: The authors declare no conflict of interest.

References

[1] Gani, A. "Fossil fuel energy and environmental performance in an extended STIRPAT model." Journal of Cleaner Production, 2021, vol. 297, 126526.

[2] Braungardt, S.; Van den Bergh, J.; Dunlop, T. "Fossil fuel divestment and climate change: Reviewing contested arguments." Energy Research & Social Science, 2019, vol. 50, pp. 191-200.

[3] Martins, F.; Felgueiras, C.; Smitkova, M. "Fossil fuel energy consumption in European countries." Energy Precedia, 2018, vol. 152, pp. 107-111.

[4] Dar, J.; Asif, M. "Environmental feasibility of a gradual shift from fossil fuels to renewable energy in India: Evidence from multiple structural breaks cointegration." Renewable Energy, 2023, vol. 202, pp. 589-601.

[5] Zeng, W.; Pang, L.; Zheng, W.; Hu, E. "Study on combustion and emission characteristics of a heavy-duty gas turbine combustor fueled with natural gas." Fuel, 2020, vol. 275, 117988.

[6] Blumberg, T.; Assar, M.; Morosuk, T.; Tsatsaronis, G. "Comparative exergoeconomic evaluation of the latest generation of combined-cycle power plants." Energy Conversion and Management, 2017, vol. 153, pp. 616–626.

[7] Carcasci, C.; Winchler, L. "Thermodynamic Analysis of an Organic Rankine Cycle for Waste Heat Recovery from an Aeroderivative Intercooled Gas Turbine." Energy Procedia, 2016, vol. 101, pp. 862-869.

[8] Gonca, G. "Exergetic and ecological performance analyses of a gas turbine system with two intercoolers and two reheaters." Energy, 2017, vol. 124, pp. 579-588.

[9] Noaman, M.; Awad, O.; Morosuk, T.; Tsatsaronis, G.; Salomo, S. "Identifying the market scenarios for supercritical CO2 power cycles." Journal of Energy Resources Technology, 2022, vol. 144(5), 050906.

[10] Liu, X.; Nguyen, M.Q.; Chu, J.; Lan, T.; He, M. "A novel waste heat recovery system combing steam Rankine cycle and organic Rankine cycle for marine engine." Journal of Cleaner Production, 2020, vol. 265, 121502.

[11] Knight, B.; Westwood, A. "World biomass review: Biomass as a global power source." Refocus, 2004, vol. 5, pp. 42–44.

[12] Toklu, E. "Biomass energy potential and utilization in Turkey." Renewable Energy, 2017, vol. 107, pp. 235-244.

[13] Cooper, N.; Panteli, A.; Shah, N. "Linear estimators of biomass yield maps for improved biomass supply chain optimization." Applied Energy, 2019, vol. 253, 113526.

[14] Molino, A.; Chianese, S.; Musmarra, D. "Biomass gasification technology: The state-of-the-art overview." Journal of Energy Chemistry, 2016, vol. 25, pp. 10–25.

[15] Habibollahzade, A.; Ahmadi, P.; Rosen, M.A. "Biomass gasification using various gasification agents: Optimum feedstock selection, detailed numerical analyses and tri-objective grey wolf optimization." Journal of Cleaner Production, 2021, vol. 284, 124718.

[16] Wu, J.; Wand, J. "Distributed Biomass Gasification Power generation system Based on Concentrated Solar Radiation." Energy Procedia, 2019, vol. 158, pp. 204–209.

[17] Narnaware, S.L.; Panwar, N.L. "Biomass gasification for climate change mitigation and policy framework in India: A review." Bioresource Technology Reports, 2022, vol. 17, 100892.

[18] Soltani, S. "Modified exergy and exergoeconomic analyses of a biomass post fired hydrogen production combined cycle." Renewable Energy, 2019, vol. 135, pp. 1466–1480.

[19] Soltani, S.; Mahmoudi, S.M.S.; Yari, M.; Morosuk, T.; Rosen, M.A.; Zare, V. "A comparative exergoeconomic analysis of two biomass and co-firing combined power plants." Energy Conversion and Management, 2013, vol. 76, pp. 83–91.

[20] Soltani, S.; Mahmoudi, S.M.S.; Yari, M.; Morosuk, T.; Rosen, M.A. "Thermodynamic analyses of an externally fired gas turbine combined cycle integrated with a biomass gasification plant." Energy Conversion and Management, 2013, vol. 70, pp. 107–115.

[21] Soltani, S.; Yari, M.; Mahmoudi, S.M.S.; Morosuk, T.; Rosen, M.A. "Advanced exergy analysis applied to an externally fired combined-cycle power plant integrated with a biomass gasification unit." Energy, 2013, vol. 59, pp. 775–780.

[22] Moharamian, A.; Soltani, S.; Rosen, M.A.; Mahmoudi S.M.S. "Advanced exergy and advanced exergoeconomic analyses of biomass and natural gas fired combined cycles with hydrogen production." Applied Thermal Engineering, 2018, vol. 134, pp. 1–11.

[23] Olgun, H.; Ozdogan, S.; Yinesor, G. "Results with a bench scale downdraft biomass gasifier for agricultural and forestry residues." Biomass and Bioenergy, 2011, vol. 35, pp. 572-580.

[24] Zainal, Z.A.; Ali, R.; Lean, C.H. "Prediction of performance of downdraft gasifier using equilibrium modeling for different biomass materials." Energy Conversion and Management, 2001, vol. 42, pp. 1499–1515.

[25] Jenkins, B.; Baxter, L.L.; Miles, T.R. "Combustion properties of biomass." Fuel Processing Technology, 1998, vol. 54, pp. 17–46.

[26] Lian, Z.T.; Chua, K.J.; Chou, S.K. "A thermoeconomic analysis of biomass energy for trigeneration." Applied Energy, 2010, vol. 87, pp. 84–95.

[27] Szargut, J.; Styrylska, T. "Approximate evaluation of exergy of fuels." Brennstoff-Wärme-Kraft, 1964, vol. 16, pp. 589–596.